Catalysis Today 252 (2015) 143–149

Contents lists available at ScienceDirect

Catalysis Today

journal homepage: www.elsevier.com/locate/cattod

Photocatalytic inactivation of *Escherichia coli* aqueous suspensions in a fixed-bed reactor

Javier Marugán[a,1], Rafael van Grieken[a], Cristina Pablos[a], M. Lucila Satuf[b], Alberto E. Cassano[b,2], Orlando M. Alfano[b,*]

[a] Department of Chemical and Environmental Technology, ESCET, Universidad Rey Juan Carlos, C/ Tulipán s/n, 28933 Móstoles (Madrid), Spain
[b] Instituto de Desarrollo Tecnológico para la Industria Química (INTEC), Universidad Nacional del Litoral-CONICET, CCT Santa Fe. Paraje El Pozo. Colectora de la Ruta Nacional No. 168, 3000 Santa Fe, Argentina

ARTICLE INFO

Article history:
Available online 16 November 2014

Keywords:
Fixed-bed reactor
Disinfection
Titanium dioxide
Monte Carlo method
Radiation absorption

ABSTRACT

A fixed-bed, annular photoreactor is studied for the photocatalytic disinfection of *Escherichia coli* aqueous suspensions. Experiments were carried out under UV radiation employing P25 titanium dioxide immobilized onto glass Raschig rings. The photoreactor performance has been simulated following a predicted procedure that takes into account explicitly the radiation absorption step and a series-event disinfection mechanism. The modeling of the radiation field was carried out by Monte Carlo simulation. The reactor model has been compared with experimental data, being able to reproduce the evolution of the concentration of viable bacteria under different bacteria initial concentrations and irradiation levels.

1. Introduction

Heterogeneous photocatalysis with titanium dioxide (TiO_2) is a well-known and effective alternative to conventional water disinfection technologies, such us chlorination, ozonization, and germicidal UV-C [1–4]. Aqueous suspensions of fine TiO_2 powder under UV irradiation are mostly employed. Nonetheless, the applicability of photocatalysis on large scale requires the immobilization of TiO_2 in order to avoid the catalyst separation step and to allow carrying out the process in continuous mode. Although the performance of immobilized systems is reported to be lower than that of TiO_2 slurry reactors in deionized water, fixed-bed reactors have shown lesser inhibition by the presence of dissolved organic matter. Besides, immobilized systems have proven to be stable and do not show deactivation after several cycles of reuse, being readily applicable for continuous water treatment systems [5].

Most of the scientific contributions on the photocatalytic inactivation of microorganisms found in the literature have proposed empirical equations or very simple models that take into account only the population of bacteria and kinetic parameters. The effect of the radiation absorption by the photocatalyst is implicitly considered in the macroscopic kinetic parameters estimated from the fitting of the experimental data. Hence, these kinetic expressions for photocatalytic bacterial inactivation are only valid for the experimental setup in which they have been developed; consequently, they cannot be extrapolated to other reactor configurations. Conversely, when a kinetic model is required for designing, optimizing or scaling-up photocatalytic reactors for water disinfection, the proposed kinetic expression must be independent of the shape and configuration of the reactor. In this case, the proposed kinetic model should be based on a reaction scheme that takes into account the radiation activated step and, explicitly, the local rate of photon absorption.

In spite of the corroborated high efficiency of fixed-bed photocatalytic reactors for water treatment, there are only a few approaches to calculate the radiation absorption in such reactors. From the numerical methods available to compute the radiation field in photocatalytic reactors, such as the discrete ordinate (DO) and the Monte Carlo (MC) methods, the latter one is chosen when complex absorption, reflection and refraction interactions between the radiation and the packed bed are involved. To the best of our knowledge, the first contribution on the modeling of a heterogeneous photoreactor using the MC method was presented by Spadoni et al. [6] for a photosensitized reaction in an annular reactor. Imoberdorf et al. [7] proposed a predictive model to solve the radiation transfer equation in a fluidized bed photocatalytic reactor, based on the MC approach coupled with the ray tracing

* Corresponding author. Tel.: +54 342 451 1546/47; fax: +54 342 451 1087.
E-mail addresses: javier.marugan@urjc.es (J. Marugán), alfano@intec.unl.edu.ar (O.M. Alfano).
[1] Tel.: +34 91 664 7466; fax: +34 91 488 7068.
[2] Deceased July 12, 2014.

http://dx.doi.org/10.1016/j.cattod.2014.10.031
0920-5861/

Nomenclature

a_v	total bacteria surface area per unit suspension volume, cm^{-1}
$a_{v,int}$	bacteria–catalyst interacting surface area per unit reactor volume, cm^{-1}
$A_{cat,R}$	total catalytic area of the reactor, cm^2
$A^{proj}_{ring,T}$	total projected area of the rings, cm^2
B	bacteria
$e^{a,s}$	local surface rate of photon absorption, einstein cm^{-2} s^{-1}
f_{int}	fraction of bacteria–catalyst interacting surface area, dimensionless
F_λ	normalized spectral distribution of the radiation emitted by the lamp, dimensionless
LSRPA	local surface rate of photon absorption, einstein cm^{-2} s^{-1}
$n_{ph,abs}$	number of photons absorbed in a spatial cell
$n_{ph,T}$	total number of photons considered in the MC simulation
P_{lamp}	emission power of the lamp, einstein s^{-1}
r	superficial reaction rate for bacteria, CFU cm^{-2} s^{-1}
R	volumetric reaction rate for bacteria, CFU cm^{-3} s^{-1}
S_{cel}	specific surface area of the bacterial cells, cm^2 CFU^{-1}
t	time, s
t_k	average thickness of the film, cm
T_f	transmission of the film, dimensionless
V	volume, cm^3
$\underline{x}$	position vector
x	rectangular coordinate, cm
z	rectangular coordinate, cm

Greek letters

α	kinetic parameter, cm $s^{-0.5}$ $einstein^{-0.5}$
α_2	kinetic parameter, dimensionless
α_3	kinetic parameter, dimensionless
θ	polar angle, rad
κ_f	volumetric absorption coefficient of the TiO_2 film, cm^{-1}
λ	radiation wavelength, nm
ξ	distance traveled by a given photon, cm
ρ	reflectivity, dimensionless
φ	azimuth angle, rad

Subscripts

0	initial condition
d	relative to damaged bacteria
i	relative to inactivated bacteria
int	relative to the bacteria–catalyst interacting surface area
p	relative to products of bacteria lysis
pi	relative to products of bacteria lysis
R	reactor
T	total
u	relative to undamaged bacteria
λ	dependence on wavelength

Special symbols

[]	concentration of bacteria species in the bulk, CFU cm^{-3}

technique. Imoberdorf et al. [8] also modeled the radiation field of a packed-bed photocatalytic reactor filled with quartz wool coated with titanium dioxide using the MC technique. Moreira et al. [9] used the MC method along with an optimization technique in a Photo-CREC annular photocatalytic reactor to estimate the wavelength-averaged absorption and scattering coefficients for three different TiO_2 powders. More recently, Zekri and Colbeau-Justin [10] applied the MC approach in a photocatalytic tubular reactor, to study the phenol degradation at different loadings of two commercial TiO_2. Also, Zazueta et al. [11] modeled the radiation field in a multi-plate photocatalytic reactor with the MC algorithm; these results were then employed to optimize the reactor design for air purification. However, most of these contributions with MC simulation were focused on the degradation of chemical contaminants and not on water disinfection.

The aim of this work is to simulate the inactivation of *Escherichia coli* in an annular photocatalytic reactor. The experiments were carried out in a laboratory scale, fixed-bed reactor filled with Raschig rings coated with TiO_2, operating in a closed recirculating system. The proposed model is based on a reaction scheme that takes into account explicitly the local surface rate of photon absorption (LSRPA) inside the reactor. Depending on the type of photocatalytic reactor under analysis, the rate of photon absorption may be expressed per unit reactor irradiated volume or per unit reactor irradiated photocatalytic surface. When modeling a fixed-bed reactor, in which a thin layer of TiO_2 is coated on the surface of an inert support, it is more appropriate to refer the photon absorption rate per unit area of irradiated TiO_2-coated surface [8]. The rate of photon absorption was computed by means of the MC simulation. Results of the LSRPA were then incorporated in the expressions of the kinetic model and the superficial disappearance rates of undamaged and damaged bacteria in the storage tank were solved to obtain their theoretical evolution as a function of time. Finally, the intrinsic kinetic parameters were estimated by applying an optimization procedure between the experimental and simulated results.

2. Experimental

2.1. The reactor

The experimental setup consists of an annular reactor 15 cm long, 3 cm inner diameter and 5 cm external diameter [12]. The reacting system was operated in a closed recirculating circuit driven by a centrifugal pump, with a stirred reservoir tank of 2 L equipped with a device for withdrawal of samples. Experiments were carried out using a total working volume of 1.0 L and a recirculation flow rate of 2.5 L/min. Illumination was carried out with a Philips TL 6W black light lamp placed in the axis of the reactor. The lamp supplies a nominal UV-A radiation power of 0.7 W with a maximum emission peak centered at 365 nm. The UV-A incident photon flow, determined by ferrioxalate actinometry, was 2.77×10^{-6} einstein s^{-1}.

The fixed-bed was prepared by immobilization of P25 TiO_2 (Evonik Industries) onto 6×6 mm glass Raschig rings and placing them into the annular photoreactor volume. Immobilization of TiO_2 has been carried out by a dip-coating procedure. The glass material was first cleaned-up with soap and water and then immersed in a KOH–isopropanol bath (200 g/L) for 24 h. The suspension consists of 150 g/L of Evonik P25 TiO_2 in deionized water at a pH value of 1.5, adjusted with HNO_3. The process was assisted by a Bungard Elektronik RDC-15 equipment working at a controlled withdrawal speed of 0.65 mm/s. After each coating cycle, the glass pieces were dried at 110 °C for 24 h and calcined at 500 °C for 2 h with a heating rate of 5 °C/min. Prior to be used in the reaction, the coated systems were mounted on the photoreactor and cleaned with water for 30 min to eliminate all the TiO_2 particles poorly adhered to the glass.

2.2. Experimental procedure

Bacterial suspensions were prepared from lyophilized *Escherichia coli* K12 strains provided by the Colección Española de Cultivos Tipo (CECT 4624, corresponding to ATCC 23631). Fresh liquid cultures with a stationary concentration of 10^9 CFU/mL were prepared by inoculation in a Luria–Bertani nutrient medium (Miller's LB Broth, Scharlab) and incubation at 37 °C for 24 h under continuous stirring on a rotary shaker. The reacting suspensions were prepared by centrifuging 5 mL of the liquid culture at 3000 rpm for 15 min, rinsing twice the bacteria with 5 mL of sterile deionized water (Milli-Q®, 18.2 MΩ cm) and finally diluting the required amount of the aqueous *E. coli* suspension to 1.0 L to get the desired initial concentration of bacteria.

All experiments have been carried out in deionized water at natural pH and room temperature. The bacterial suspension was charged in the reservoir tank and the centrifugal pump was switched on to drive the recirculation flow rate. The system was equilibrated for 15 min and, in the meantime, the lamp was switched on outside the reactor to stabilize its emission power and spectrum before the reaction starts.

The bacterial inactivation was followed by analyzing the concentration of viable bacteria in the samples taken along the reaction. The quantification was carried out following a standard serial dilution procedure, spotting 10 μL of each decimal dilution eight times on LB nutrient agar plates (Miller's LB Agar, Scharlab) and incubating them at 37 °C for 24 h before counting. For high irradiation times (low bacterial concentrations) higher volumes of 100 μL and 1 mL of the undiluted suspension were also plated to reduce the detection limit to 1 CFU/mL. Experiments were carried out with different initial bacterial concentrations (10^6–10^3 CFU/mL) and different irradiation levels (100, 80, and 60%). These levels were obtained by interposing neutral filters between the lamp and the inner wall of the reactor.

3. Reactor modeling

3.1. Mass balances

The small reactor volume and the relatively slow reaction rates of the disinfection process allow the following assumptions: (i) the system is perfectly mixed, (ii) there are no mass transport limitations, (iii) the conversion per pass in the annular reactor is differential, and (iv) parallel dark reactions are neglected. Consequently, the mass balances and initial conditions of undamaged and damaged bacteria in the storage tank are given by:

$$\frac{d[B_u](t)}{dt} = -\frac{V_R}{V_T}\left\langle R_u(\underline{x}, t)\right\rangle_{V_R} \quad (1)$$

$$t = 0, \quad [B_u] = [B_u]_0 \quad (2)$$

$$\frac{d[B_d](t)}{dt} = \frac{V_R}{V_T}\left[\left\langle R_u(\underline{x}, t)\right\rangle_{V_R} - \left\langle R_d(\underline{x}, t)\right\rangle_{V_R}\right] \quad (3)$$

$$t = 0, \quad [B_d] = 0 \quad (4)$$

where $[B_u]$ and $[B_d]$ are the concentration of undamaged and damaged bacteria, respectively, $[B_u]_0$ the initial concentration of bacteria, V_R the irradiated reactor volume, V_T the total suspension volume, t the reaction time, and $\left\langle R_i(\underline{x}, t)\right\rangle_{V_R}$ the volumetric inactivation rate of undamaged (i = u) and damaged (i = d) bacteria averaged over the whole reactor volume.

The kinetic model for the photocatalytic disinfection of bacteria proposed in Section 3.2 is based on a superficial disappearance rate of bacteria. Accordingly, the volumetric disappearance rates of undamaged (R_u) and damaged bacteria (R_d) considered in Eqs. (1) and (3), should be transformed into the corresponding superficial disappearance rates of undamaged (r_u) and damaged (r_d) bacteria by the equations [13]:

$$R_u\left(\frac{CFU}{s\ cm^3}\right) = r_u\left(\frac{CFU}{s\ cm^2_{int}}\right) a_{v,int}\left(\frac{cm^2_{int}}{cm^3}\right) = r_u f_{int} a_v = r_u f_{int} S_{cel}\,[B_u] \quad (5)$$

$$R_d\left(\frac{CFU}{s\ cm^3}\right) = r_d\left(\frac{CFU}{s\ cm^2_{int}}\right) a_{v,int}\left(\frac{cm^2_{int}}{cm^3}\right) = r_d f_{int} a_v = r_d f_{int} S_{cel}\,[B_d] \quad (6)$$

where $a_{v,int}$ is the bacteria–catalyst interacting surface area per unit reactor volume, f_{int} the fraction of bacteria–catalyst interacting surface area, a_v the total bacteria surface area per unit suspension volume, and S_{cel} the specific surface area of the bacterial cells. Notice that for a fixed-bed, photocatalytic reactor packed with glass rings, f_{int} is the fraction of useful surface area of the rings.

3.2. Kinetic model

The photocatalytic inactivation of *E. coli* is modeled in a simple way by a reaction scheme which involves a series events in which bacteria are gradually damaged and finally led to cell lysis [14,15]. The reaction scheme includes the following steps: activation of the catalyst by radiation of the required wavelength to form the electron–hole pair; recombination of electrons and holes; electrons trapping, having molecular oxygen as the main electron acceptor; and holes trapping by adsorbed species. It is proposed that hydroxyl radicals, generated by the holes trapping step, can attack undamaged (B_u), damaged (B_d) and inactivated (B_i) population of bacteria. Finally, the attack of hydroxyl radicals to inactivated bacteria leads to the formation of B_{pi} (with i = 1 to n), which represents biological structures and compounds released after the cell lysis. It has been experimentally verified that direct photolysis of *E. coli* suspensions under UV-A irradiation in the 340–400 nm wavelength range was negligible in comparison with the photocatalytic inactivation. No significant changes in the concentration of viable bacteria were found without the addition of the photocatalyst [12,14].

In a previous work, a kinetic model has been developed based on the proposed reaction scheme and accounting explicitly for the rate of photon absorption [15]. Following a similar procedure, the superficial disappearance rates of undamaged and damaged bacteria, under high irradiation conditions, are given by the expressions:

$$r_u\left(\frac{CFU}{s\ \ cm^2}\right) = \alpha_1 \frac{[B_u]}{[B_u] + \alpha_2[B_d] + \alpha_3\,([B_u]_0 - [B_u] - [B_d])}\sqrt{e^{a,s}(\underline{x})} \quad (7)$$

$$r_d\left(\frac{CFU}{s\ \ cm^2}\right) = \alpha_1 \frac{\alpha_2[B_d]}{[B_u] + \alpha_2[B_d] + \alpha_3\,([B_u]_0 - [B_u] - [B_d])}\sqrt{e^{a,s}(\underline{x})} \quad (8)$$

where $e^{a,s}$ is the LSRPA and α_1, α_2 and α_3 are lumped kinetic parameters. It should be noted that the proposed kinetic model gives a general rate expression with an explicit dependence of the radiation absorption effects on the bacterial inactivation rate.

To obtain the volumetric reaction rate, Eqs. (7) and (8) are introduced into Eqs. (5) and (6), respectively:

$$R_u\left(\frac{CFU}{s\ cm^3}\right) = \alpha \frac{[B_u]^2}{[B_u] + \alpha_2[B_d] + \alpha_3\,([B]_0 - [B_u] - [B_d])}\sqrt{e^{a,s}(\underline{x})} \quad (9)$$

$$R_d\left(\frac{\text{CFU}}{\text{s cm}^3}\right) = \alpha \frac{\alpha_2[B_d]^2}{[B_u]+\alpha_2[B_d]+\alpha_3\left([B]_0-[B_u]-[B_d]\right)}\sqrt{e^{a,s}(\underline{x})} \quad (10)$$

where $\alpha = \alpha_1 f_{int} S_{cel}$.

4. Evaluation of the radiation absorption

The MC method has been applied to obtain the distribution of the absorbed radiation at each point in the fixed-bed reactor. In general terms, the MC method applied to the radiation field resolution consists of tracking the trajectory of a great number of photons until they are either absorbed or lost. Inside the reactor, photons travel with a linear trajectory in the aqueous phase until they reach a TiO_2-coated ring, the reactor windows, or the reactor walls. Those photons that reach the rings can be either reflected by the catalytic surface, absorbed by the TiO_2 film, or transmitted. Once every photon is tracked and the point of its probable absorption is stored, it is possible to calculate the rate of photon absorption inside the photocatalytic reactor.

The following assumptions have been adopted in the radiation model:

(i) The lamp is considered as a linear source, with uniform emission along its length and directionally independent.
(ii) Photons that travel through the air space between the lamp and the reactor inner wall follow a linear trajectory, without interaction with the medium.
(iii) Reflection, refraction and absorption in the reactor windows are neglected.
(iv) Inside the reactor, photons travel linearly until they reach a coated ring.
(v) When a photon bundle hits a coated ring, it can be reflected, absorbed or transmitted.
(vi) The light reflection on the TiO_2 film is considered specular [16].
(vii) The transmittance of the TiO_2 film is evaluated by considering the spectral volumetric absorption coefficient of the coating and the average thickness of the film.
(viii) Refraction and reflection by the glass walls of the rings is neglected, i.e. only the properties of TiO_2 film are considered.
(ix) Photons that reach the top, bottom or non-irradiated reactor walls are assumed lost, and a new photon bundle is considered.

Due to the circular symmetry of the annular reactor, two spatial coordinates were employed [6]: x and z. Therefore, the annular reaction region was divided into 2D spatial cells to store the absorption place of the photons. The emission range of the lamp, from 350 to 400 nm, was discretized into six wavelengths (every 10 nm). The simulation involved the tracking of 10^7 photon bundles for each wavelength. It was verified that a greater number of photons did not introduce variations in the computed results of photon absorption profiles inside the reactor. Fig. 1 shows a schematic representation of the reactor annular region and the coordinate system employed in the radiation model.

A flowchart of the MC algorithm followed to solve the radiation model is presented in Fig. 2.

The first step in the simulation is the emission of a photon bundle by the lamp. One random number (R_1) is generated to establish the emission point e_p along the lamp (e_p = lamp length × R_1). Another random number is set to define the polar angle of the trajectory: $\theta = a\sin(2R_2 - 1)$ (owing to the cylindrical symmetry, the azymuth angle φ is automatically assigned). After the direction of the flight has been defined, the photon bundle travels along the air space between the lamp and the reactor window with a linear trajectory. According to the emission position and the direction of the flight, photons can reach the reactor or escape through the top or the bottom of this space. If the photon bundle reaches the fixed-bed, it travels a distance ξ without interaction. The value of ξ is computed by a random number R_3 as $\xi = -\text{MFP}\ln(R_3)$, where MFP is the mean free path of photons inside the reactor. MFP can be estimated as $\text{MFP} = V_R/A^{proj}_{ring,T}$. $A^{proj}_{ring,T}$ stands for the total sum of the projected area of the rings [17]. The new location of the photon bundle, after traveling distance ξ is computed as $x_{new} = x_{old} + e_x\xi$ and $z_{new} = z_{old} + e_z\xi$, where the subscript old refers to the previous position and the subscript new indicates the new location. e_x and e_z represent the direction cosines with respect to the coordinate axis. In the new position, the photon bundle is considered to reach a coated ring. The orientation of the ring and the location of the interception point on the ring wall are stochastically assigned by two new random numbers R_4 and R_5. Three events can then take place: reflection, absorption or transmission. The local reflectivity ρ is calculated using the Fresnel equation. If a random number $R_6 < \rho$, photons are reflected. The direction of the reflected photons is determined considering specular reflection. If $R_6 > \rho$, the transmission of the TiO_2 film ($T_{f,\lambda}$) is evaluated as $T_{f,\lambda} = \exp(-\kappa_{f,\lambda}t_k)$, where $\kappa_{f,\lambda}$ is the spectral volumetric absorption coefficient of the film and t_k the average thickness. The values of $\kappa_{f,\lambda}$ and t_k were obtained from a previous study [15]. By comparing $T_{f,\lambda}$ with another random number, it is possible to determine the fate of the photon bundle. If $R_T > T_{f,\lambda}$, photons are absorbed and the absorption position is stored. Otherwise, photons are transmitted, reaching an internal wall of the ring or the liquid phase. This sequence continues until all the photon trajectories are tracked.

The LSRPA for each wavelength, $e^{a,s}_\lambda(x,z)$, is calculated according to

$$e^{a,s}_\lambda(x,z) = \frac{n_{ph\lambda,abs}(x,z)}{n_{ph\lambda,T}} \frac{F_\lambda P_{lamp}}{2\pi r \Delta x \Delta z} \frac{V_R}{A_{cat,R}} \quad (11)$$

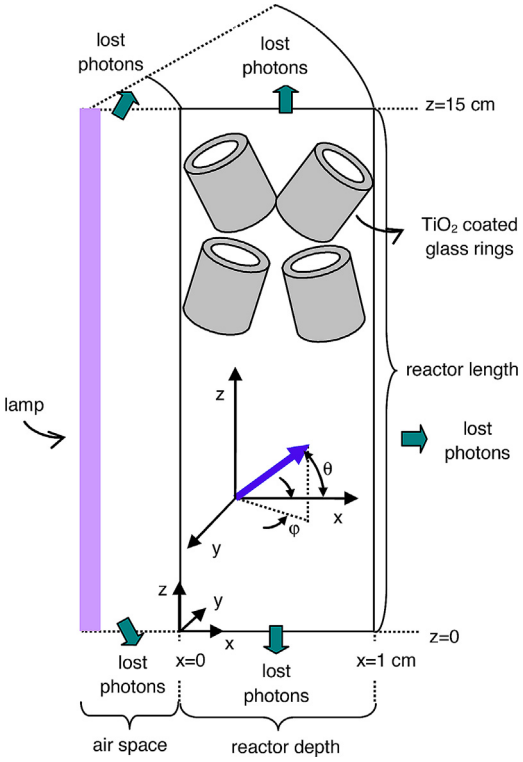

Fig. 1. Schematic representation of the reactor and coordinate system.

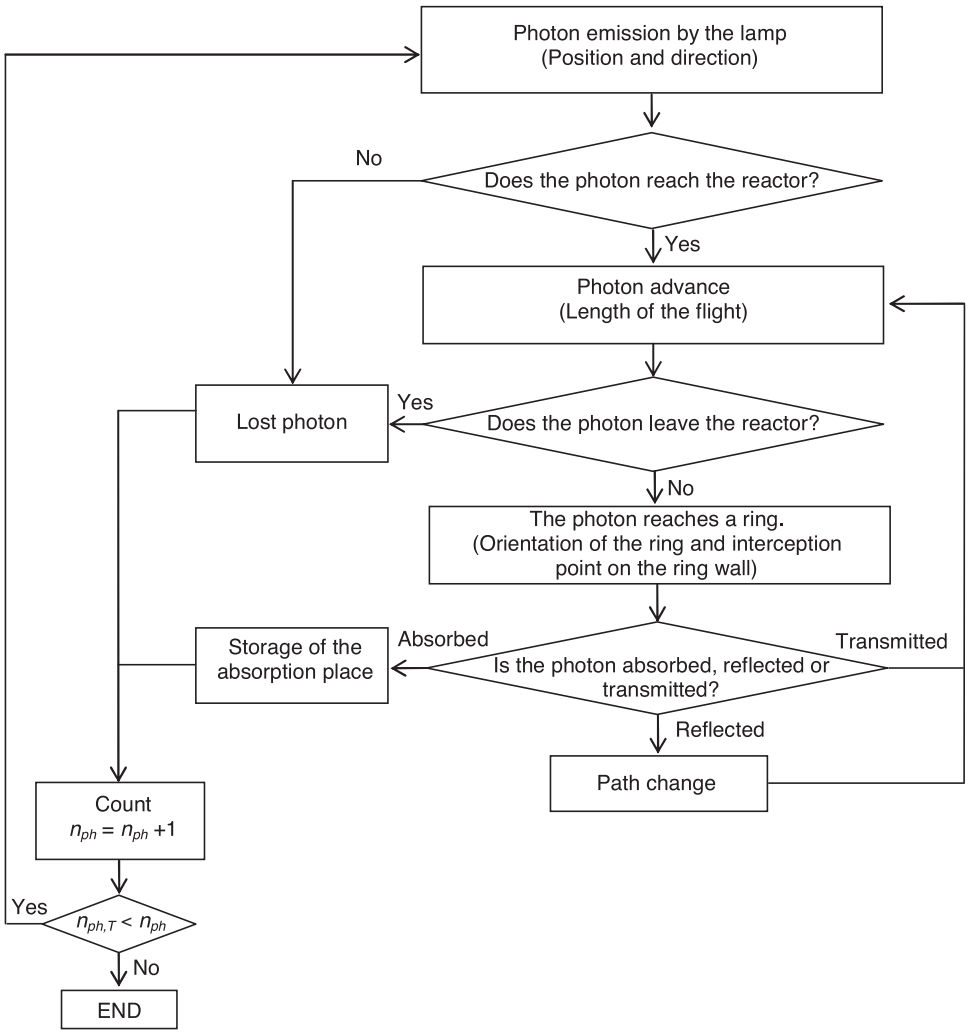

Fig. 2. Flowchart of the MC algorithm.

where $n_{ph\lambda,abs}(x, z)$ is the number of photons of wavelength λ absorbed in the spatial cell corresponding to the coordinates (x, z), $n_{ph\lambda,T}$ the total number of photons of wavelength λ considered in the simulation, P_{lamp} the emission power of the lamp, F_λ the normalized spectral distribution of the radiation emitted by the lamp (given by the manufacturer), r the distance between the spatial cell and the center of the reactor, Δx and Δz correspond to the cell dimensions, and $A_{cat,R}$ the catalytic area of the reactor. $A_{cat,R}$ is calculated taking into account the sum of the external and internal areas of the total coated rings.

Finally, the LSRPA considering the whole wavelength range emitted by the lamp is calculated as:

$$e^{a,s}(x, z) = \sum_{\lambda=350nm}^{\lambda=400nm} e_\lambda^{a,s}(x, z) \quad (12)$$

Fig. 3 shows the absorption distribution in the fixed-bed reactor obtained with the Monte Carlo simulation, employing rings with two TiO_2 coatings.

5. Experimental and simulated results

Previous experiments have shown that the optimum number of catalyst coatings on the rings was two. One coating rendered lower inactivation rates, and three coatings did not improve the performance obtained with two. Therefore, all the experiments employed

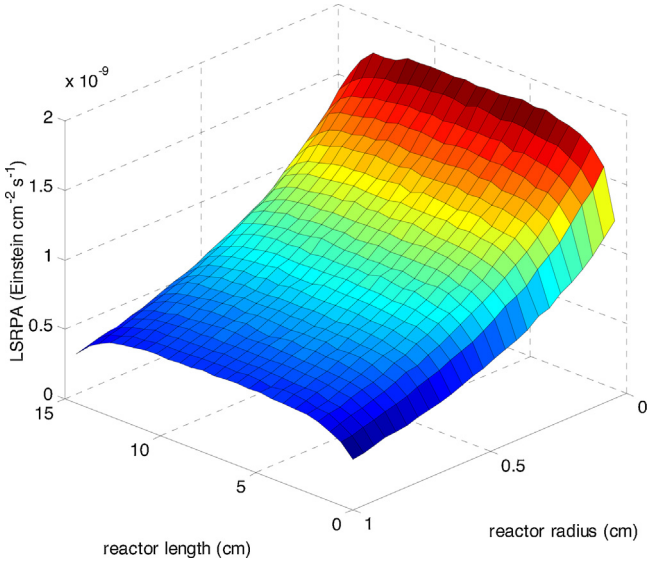

Fig. 3. Local rate of photon absorption as a function of the reactor radius and length, employing rings with two TiO_2 coatings.

Table 1
Estimated kinetic parameters.

Parameter	α	α_2	α_3
Value	2.42×10^3	8.09×10^{-10}	≅0
Confidence interval (95%)	$\pm 0.29 \times 10^3$	$\pm 3.20 \times 10^{-10}$	–
Units	cm $s^{-0.5}$ einstein$^{-0.5}$	Dimensionless	Dimensionless

to estimate the kinetic parameters were carried out with rings containing two coatings of TiO_2.

The resolution of the mass balance equations (Eqs. (1)–(4)) renders the changes in the concentration of *E. coli* in the reservoir tank as a function of the irradiation time. These values can be compared with the experimental results considering that undamaged and damaged bacteria remain viable and consequently both can be counted by the plating technique.

Kinetic parameter defined in Eqs. (9) and (10) was estimated by means of the Levenberg–Marquardt optimization algorithm. The final values of the kinetic parameters, with the corresponding 95% confidence interval, are reported in Table 1.

Figs. 4 and 5 show the experimental and simulated profiles of inactivation obtained for *E. coli* suspension under different experimental conditions. Two different regions can be clearly identified: (i) a smooth decay at the beginning of the reaction, usually called "shoulder"', followed by (ii) a log-linear region, where rapid bacterial inactivation takes place. Similar profiles have been previously reported in the literature [14,15,18]. The presence of the shoulder can be explained by considering that the damage to the bacterial cells produced by •OH radicals generated upon irradiation of TiO_2 is cumulative rather than instantly lethal. During the first minutes of irradiation, •OH radicals begin to attack the membrane but not sufficiently to cause serious damage. The microorganisms resist this attack with self-defense and auto-repair mechanisms. During the log-linear period, microorganism inactivation is accelerated. The anti-stress enzymes are no longer able to protect the bacterial membrane and, hence, membrane perforation can occur. The length of the shoulder region in the inactivation curves would depend on the rate of •OH radicals, which in turn depends on the rate of photon absorption. Higher irradiation levels produce higher rates of photon absorption and •OH radicals, reducing the length of the initial shoulder and increasing the slope of the log-linear deactivation region. This effect can be clearly observed in Fig. 4.

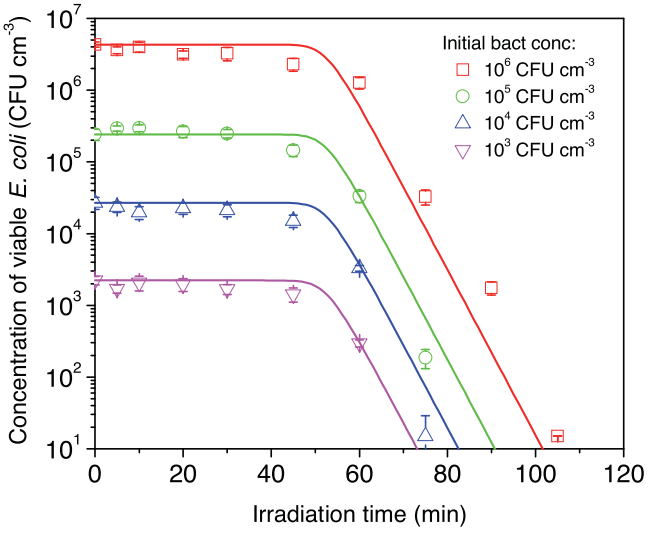

Fig. 4. Photocatalytic inactivation of *E. coli* suspensions with different initial concentrations of bacteria. Symbols: experimental data; solid lines: model.

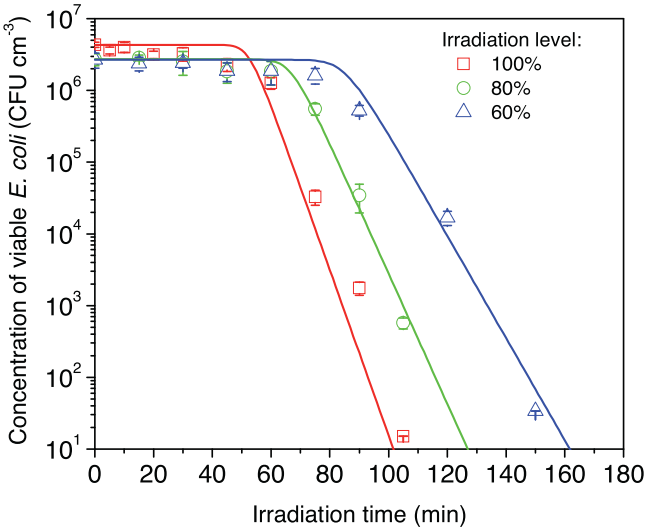

Fig. 5. Photocatalytic inactivation of *E. coli* suspensions with different irradiation levels. Symbols: experimental data; solid lines: model.

From Figs. 4 and 5, it can be concluded that the model is able to satisfactorily simulate the evolution of the concentration of viable bacteria in the fixed-bed reactor under different experimental conditions, achieving a root mean square logarithmic error of 0.305.

Finally, from the photocatalytic disinfection results obtained in the fixed-bed reactor, two types of inactivation efficiencies can be evaluated: the photonic efficiency and the quantum efficiency. The photonic efficiency (η_p) is defined as the ratio of the total amount of inactivated bacteria during a given time to the total number of photons arriving at the reactor wall during the same period of time. The following results are obtained: $\eta_p = 5.11 \times 10^{-13}$ CFU/photon for an initial concentration of bacteria of 1.0×10^6 CFU cm^{-3} and $\eta_p = 3.95 \times 10^{-15}$ CFU/photon for an initial concentration of bacteria of 1.0×10^4 CFU cm^{-3}. On the other hand, the quantum efficiency (η_q) is defined as the ratio of the total amount of inactivated bacteria during a given time to the total number of photons absorbed in the reactor during the same period of time. In this case, the following results are found: $\eta_q = 2.61 \times 10^{-12}$ CFU/photon for an initial concentration of bacteria of 1.0×10^6 CFU cm^{-3} and $\eta_q = 2.02 \times 10^{-14}$ CFU/photon for an initial concentration of bacteria of 1.0×10^4 CFU cm^{-3}.

6. Conclusions

The photocatalytic inactivation of *Escherichia coli* has been modeled by means of a series-event disinfection scheme that involves the explicit radiation absorption rates of the P25 titanium dioxide immobilizated onto glass Raschig rings. The local rate of photon absorption was calculated by means of the Monte Carlo simulation. The experiments were carried out in a fixed-bed, annular photoreactor filled with Raschig rings, operating in a recirculation batch mode.

From the comparison of the simulated results with the experimental data, it can be concluded that the proposed model is able to satisfactorily simulate the evolution of the concentration of viable bacteria in the fixed-bed reactor under different bacteria initial concentrations and irradiation levels.

Acknowledgments

The authors gratefully acknowledge the financial support of the Spanish Ministry of Economy and Competitiveness (MINECO) through the project EMBIOPHOTO (CTM2011-29143-C03-01)

and Comunidad de Madrid through the program REMTAVARES (S2009/AMB-1588). Also, they acknowledge the financial support from the Universidad Nacional del Litoral, Agencia Nacional de Promoción Científica y Tecnológica, and Consejo Nacional de Investigaciones Científicas y Técnicas of Argentina. Cristina Pablos acknowledges Ministerio de Ciencia e Innovación for the FPU grant (AP2008-04567).

References

[1] A.G. Rincón, C. Pulgarin, Appl. Catal. B: Environ. 44 (2003) 263–284.
[2] C. McCullagh, J.M.C. Robertson, D.W. Bahnemann, P.K.J. Robertson, Res. Chem. Intermed. 33 (2007) 359.
[3] S. Malato, P. Fernández-Ibáñez, M.I. Maldonado, J. Blanco, W. Gernjak, Catal. Today 147 (2009) 1–59.
[4] M.N. Chong, B. Jin, C.W.K. Chow, C. Sant, Water Res. 44 (2010) 2997.
[5] C. Pablos, R. van Grieken, J. Marugán, B. Moreno, Catal. Today 161 (2011) 133–139.
[6] G. Spadoni, E. Bandini, F. Santarelli, Chem. Eng. Sci. 33 (1978) 517–524.
[7] G.E. Imoberdorf, F. Taghipour, M. Keshmiri, M. Mohseni, Chem. Eng. Sci. 63 (2008) 4228–4238.
[8] G.E. Imoberdorf, G. Vella, A. Sclafani, L. Rizzuti, O.M. Alfano, A.E. Cassano, AIChE J. 56 (2010) 1030–1044.
[9] J. Moreira, B. Serrano, A. Ortíz, H. de Lasa, Chem. Eng. Sci. 66 (2011) 5813–5821.
[10] M. Zekri, C. Colbeau-Justin, Chem. Eng. J. 225 (2013) 547–557.
[11] A.L.L. Zazueta, H. Destaillats, G. Li Puma, Chem. Eng. J. 217 (2013) 475–485.
[12] R. van Grieken, J. Marugán, C. Sordo, C. Pablos, Catal. Today 144 (2009) 48–54.
[13] J. Marugán, R. van Grieken, C. Pablos, M.L. Satuf, A.E. Cassano, O.M. Alfano, Appl. Catal. B: Environ. 102 (2011) 404–416.
[14] J. Marugán, R. van Grieken, C. Sordo, C. Cruz, Appl. Catal. B: Environ. 82 (2008) 27–36, Corrigendum: *Appl. Catal. B: Environ.* 88 (2009) 582–583.
[15] J. Marugán, R. van Grieken, C. Pablos, M.L. Satuf, A.E. Cassano, O.M. Alfano, Catal. Today 240 (2015) 9–15.
[16] G.E. Imoberdorf, O.M. Alfano, A.E. Cassano, H.A. Irazoqui, AIChE J. 53 (2007) 2688–2703.
[17] G. Vella, G.E. Imoberdorf, A. Sclafani, A.E. Cassano, O.M. Alfano, L. Rizzuti, Appl. Catal. B: Environ. 96 (2010) 399–407.
[18] A.K. Benabbou, Z. Derriche, C. Felix, P. Lejeune, C. Guillard, Appl. Catal. B: Environ. 76 (2007) 257–263.